J Appl Physiol 107: 549–557, 2009.
First published May 28, 2009; doi:10.1152/japplphysiol.00280.2009.

A transient antioxidant stress response accompanies the onset of disuse atrophy in human skeletal muscle

Luciano Dalla Libera,[1] Barbara Ravara,[2] Valerio Gobbo,[1] Elena Tarricone,[2] Maurizio Vitadello,[1] Gianni Biolo,[3] Giorgio Vescovo,[4] and Luisa Gorza[2]

[1]*Consiglio Nazionale delle Ricerche-Institute for Neuroscience, and* [2]*Department of Biomedical Sciences, University of Padova, Padova;* [3]*Department of Clinical, Technological and Morphological Sciences, Division of Internal Medicine, University of Trieste, Trieste; and* [4]*Division of Internal Medicine, San Bortolo Hospital, Vicenza, Italy*

Submitted 16 March 2009; accepted in final form 22 May 2009

Dalla Libera L, Ravara B, Gobbo V, Tarricone E, Vitadello M, Biolo G, Vescovo G, Gorza L. A transient antioxidant stress response accompanies the onset of disuse atrophy in human skeletal muscle. *J Appl Physiol* 107: 549–557, 2009. First published May 28, 2009; doi:10.1152/japplphysiol.00280.2009.—It is presently unknown whether oxidative stress increases in disused skeletal muscle in humans. Markers of oxidative stress were investigated in biopsies from the vastus lateralis muscle, collected from healthy subjects before [*time 0* (T0)], after 1 wk (T8), and after 5 wk (T35) of bed rest. An 18% decrease in fiber cross-sectional area was detected in T35 biopsies ($P < 0.05$). Carbonylation of muscle proteins significantly increased about twofold at T35 ($P < 0.02$) and correlated positively with the decrease in fiber cross-sectional area ($P = 0.04$). Conversely, T8 biopsies showed a significant increase in protein levels of heme oxygenase-1 and glucose-regulated protein-75 (Grp75)/mitochondrial heat shock protein-70, two stress proteins involved in the antioxidant defense ($P < 0.05$). Heme oxygenase-1 increase, which involved a larger proportion of slow fibers compared with T0, appeared blunted in T35 biopsies. Grp75 protein level increased threefold in T8 biopsies and localized especially in slow fibers ($P < 0.025$), to decrease significantly in T35 biopsies ($P < 0.05$). Percent change in Grp75 levels positively correlated with fiber cross-sectional area ($P = 0.01$). Parallel investigations on rat soleus muscles, performed after 1–15 days of hindlimb suspension, showed that Grp75 protein levels significantly increased after 24 h of unloading ($P = 0.02$), i.e., before statistically significant evidence of muscle atrophy, to decrease thereafter in relation to the degree of muscle atrophy ($P = 0.03$). Therefore, in humans as in rodents, disuse muscle atrophy is characterized by increased protein carbonylation and by the blunting of the antioxidant stress response evoked by disuse.

bed rest; protein carbonylation; heme oxygenase-1; glucose-related protein-75; hindlimb suspension

BED-REST IMMOBILIZATION IS common in patients as an integral part either of diseases or of their treatment, and experimental bed rest represents a well-accepted analog of inactivity-induced body deconditioning (see Ref. 34, as an extensive review). Long-term bed rest induces several systemic alterations, among which are bone loss, muscle atrophy, and reduced muscle strength (7, 34). In humans, the antigravity muscles of the lower and upper limbs (soleus, gastrocnemius, and vastus lateralis) are the most affected by exposure to real and simulated microgravity (1, 11, 34). Changes in muscle size and strength of these muscles have been studied after bed rest of various durations (1, 34). After 5 wk of bed rest, gastrocnemius medialis and vastus lateralis muscles showed significant atrophy (1, 5, 11), and, parallel to the decline in myofibrillar protein content, single myofibers isolated from biopsies obtained from vastus lateralis muscle showed a 40% decrease in the development of specific tension [maximum force normalized to cross-sectional area (CSA)] (24).

In addition to increased protein catabolism and reduced protein synthesis (38, 45), impaired muscle force production accompanying skeletal muscle atrophy may also be the consequence of oxidative changes occurring at the level of myofibrillar proteins (9). Extensive carbonylation of myosin heavy chains (MHC), actin, and tropomyosin, revealed by means of the Oxyblot assay, was observed in the presence of hindlimb muscle atrophy accompanying heart failure, both in the laboratory rat and in patients (9, 50). The same myofibrillar proteins were also the targets of oxidative changes in respiratory muscles of patients affected with chronic obstructive pulmonary disease (29) and in postischemic-reperfused rat hearts (47). In skeletal muscle atrophy of patients affected with heart failure, the extent of oxidation of skeletal myofibrillar proteins showed a negative correlation with exercise capacity, measured as oxygen consumption at maximum exercise (peak $\dot{V}O_2$) (50). Several studies in experimental animals indicated that oxidative injury occurred after disuse of locomotor skeletal muscles, through the demonstration of increased protein carbonylation (3, 21) or imbalance of the expression of antioxidant enzymes (23, 45; Refs. 4 and 36, as reviews). The source of reactive oxygen species (ROS) in the inactive muscle remains still undetermined (36). Although several oxidant production pathways, such as xanthine oxidase, NADPH-oxidase, and mitochondria, might contribute to superoxide production in muscle fibers, a growing body of evidence showed that intracellular free iron increased in atrophied muscles (17, 22), favored by dysregulation of iron homeostasis (17, 45), and thus enhancing the production of hydroxyl radicals and metabolites of biooxidation. Subsequent effects on calcium homeostasis and on the production of nitric oxide by nitric oxide synthase might promote further the formation of reactive species and contribute to the functional depression of muscle contractility and force production, as suggested by the observed increase in *S*-nitrosylation of the calcium channel/ryanodine receptor type 1 in human soleus muscle after 55 day of bed rest (39). Alternatively, ROS increase might result from the decreased production of endogenous antioxidant defenses (8, 25, 44, 45), due to the decrease in protein synthesis accompanying muscle atrophy (38, 45).

Another, albeit indirect, proof that oxidative injury accompanied muscle disuse in the hindlimb-suspended rat was pro-

Address for reprint requests and other correspondence: L. Gorza, Dept. of Biomedical Sciences, Viale G. Colombo 3, 35121 Padova, Italy (e-mail: luisa.gorza@unipd.it).

vided by the finding of an antioxidant stress response, characterized by the expression of the inducible heme oxygenase-1 isoform (HO-1) (18), a small heat shock protein (Hsp), detectable at low levels in skeletal muscle (46). HO-1 is highly induced by ROS and by heme, acts as a controller of the intracellular iron homeostasis, and exerts an antioxidant protection through the release of biliverdin and carbon monoxide (31, 37).

Due to the lack of comparable evidence for human muscle (4), the present study was aimed to investigate whether disuse alone, or simulated microgravity, was accompanied by the occurrence of oxidative stress and/or changes in the expression of proteins involved in the antioxidant defense. To this purpose, the bed-rest protocol provides a meaningful opportunity to define some of the events that might favor either the initiation or the progression of muscle atrophy in humans.

This investigation was conducted within a 5-wk bed-rest study, during which three sequential muscle biopsies were obtained from the same healthy subject. Such an approach allowed us to monitor the development of muscle atrophy and to evaluate the presence and the degree of protein oxidation and antioxidant stress response.

Therefore, muscle biopsies obtained from human vastus lateralis were analyzed to monitor changes in fiber CSA, protein carbonylation, and expression of HO-1. We also investigated changes in protein levels of the Hsp glucose-regulated protein-75 (Grp75), i.e., the mitochondrial Hsp70 isoform (20), which is upregulated by oxidative stress like HO-1 (30) and, in addition to several other functions (i.e., mitochondrial import, antigen processing, control of cell proliferation and differentiation), exerts antioxidant cytoprotection (20), insofar as its overexpression in PC12 cells significantly reduced ROS accumulation due to glucose deprivation (27). Because the presence of disuse-induced changes in muscle Grp75 expression was never addressed in experimental animal models, we extended our investigation to soleus muscles of hindlimb-suspended rats.

MATERIALS AND METHODS

Human biopsies. The bed-rest campaign was organized in July 2007, at the Orthopaedic Hospital of Valdoltra (Koper, Slovenia), by the working group on Osteoporosis and Muscle Atrophy of the Italian Space Agency, and the University of Primorska, Science and Research Center of Koper (Slovenia). The protocol was in accordance with the principles of the Helsinki Declaration, the Oviedo Convention on Human Rights and Biomedicine, and the Slovene Code of Medical Deontology and was approved by the ethical committee of the University of Primorska. Written, informed consent was obtained from all of the participants before the beginning of the study. Ten healthy, male subjects (mean ± SE age: 24 ± 1 yr; body weight: 78 ± 3 kg) participated in the study. All volunteers were untrained before admission, and the presence of chronic or acute diseases was excluded. All subjects received identical nutrition calculated on the basis of prestudy body weights, in accordance with Refs. 6 and 28. The day before the start of bed rest, participants underwent a biopsy from the vastus lateralis muscle [*time 0* (T0)]. Subsequent biopsies were obtained from the contralateral muscle after 7 days [time 8 days (T8)] and 5 wk [time 35 days (T35)] of bed rest, performed without head-down tilt. After local anesthesia, the muscle biopsy was taken in sterile conditions, according to standard techniques; muscle fibers were immediately cleaned from visible fat or connective tissue and gently dried to remove visible blood. From each biopsy, a sample of ~20 mg was removed, frozen in liquid nitrogen, and stored at −80°C for this study. T35 muscle biopsy of *subject 2* (S2) failed for technical reasons, and T8 sample of S1 corresponded to a blood clot devoid of muscle fibers.

Morphometric and immunohistochemical analyses. Serial consecutive 12-μm cryosections were prepared from frozen muscle biopsies and assayed for hematoxylin-eosin and indirect peroxidase immunohistochemistry, following previously described protocols (46, 49). Fiber CSA was calculated with a computerized interactive method (Scion Image, NIH, Bethesda, MD) and expressed in micrometers squared by evaluating at least 100 transversely cut fibers. Fiber typing was achieved by means of indirect immunoperoxidase staining. Sections were incubated overnight at 4°C with the following mouse monoclonal anti-MHC antibodies, raised as described in Ref. 40: BA-D5, which reacts with β-MHC isoform and recognizes type 1 fibers (15–16); BF-13, which stains all type 2 fibers (43); BF-35, which, in humans, reacts with both β- and 2A-MHC isoforms and recognizes type 1 and 2A fibers (42–43), and, therefore, allows the identification of unreactive fibers as fast 2X fibers, i.e., the "old" histochemical type 2B ones. After adequate rinses with PBS, sections were incubated with appropriate dilutions of goat anti-mouse immunoglobulins, conjugated with peroxidase (sc-2055; Santa Cruz Biotech, Heidelberg, Germany) and then revealed with diaminobenzidine. Sections stained for fiber typing were also used for CSA measurements. For stress protein immunolocalization, cryosections from the biopsies of a same subject were collected on a single slide and labeled

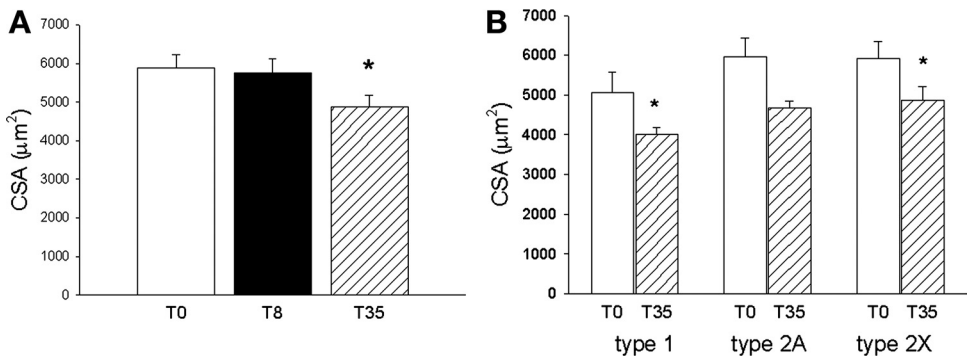

Fig. 1. Bed rest-induced changes in fiber cross-sectional area (CSA) of vastus lateralis muscle. *A*: histograms show means and SE of fiber CSA values measured in vastus lateralis muscle biopsies obtained from 7 subjects before [*time 0* (T0)] and after 8 days (T8) or 35 days (T35) of bed rest. An average of 100 fibers was evaluated for each biopsy. Two subjects [*subjects 1* and *2* (S1 and S2)] lacked one biopsy for technical reasons, as described in MATERIAL AND METHODS, and two biopsies from S6 could not be evaluated because of the absence of transversally cut fibers (see Supplemental Table 1). *Significant difference ($P < 0.05$; within-subjects ANOVA). *B*: histograms show means and SE of fiber CSA detected for each fiber-type population in T0 and T35 biopsies from subjects S1, S7, S8, and S10 (average no. of fibers examined for each biopsy = 150). *Significant difference vs. the corresponding T0 value ($P \leq 0.05$, paired Student's *t*-test).

Table 1. *Percentages of type 1, 2A, and 2X fibers in T0 and T35 vastus lateralis biopsies*

	Type 1	Type 2A	Type 2X
T0	30.74±3.33	41.27±2.94	27.74±2.40
T35	29.01±2.93	45.15±3.74	26.08±5.17

Values are means ±SE in %total (percentages of each fiber-type population on total fiber number); $n = 8$ subjects. Average no. of fibers evaluated for each biopsy = 200. T0, *time 0*, before bed rest; T35, after 35 days of bed rest. Comparison of T0 vs. T35 values was performed with paired Student's *t*-test. $P = 0.57$ for type 1; $P = 0.46$ for type 2A; $P = 0.78$ for type 2X.

using indirect peroxidase staining with either anti-Grp75 mouse monoclonal antibody diluted 1:400 (SPS-825; Stressgen, Victoria, BC) or with a 1:20 dilution of anti-HO-1 goat polyclonal antibody (sc-1797; Santa Cruz Biotechnology) (46). Positive and negative fibers were determined by visual inspection on micrographs taken using the same light intensity and exposure time. Evaluation of the presence or the absence of fiber staining was performed independently by two investigators.

Oxyblot procedure and Western blot analysis. The presence of protein carbonyl groups was assessed using the Oxyblot protein oxidation detection kit (Millipore, Vimodrone, Italy), according to the manufacturer's protocol. About 20 cryosections (12 μm) were solubilized, as previously described (9), and 6 μg of protein were used for derivatization with 2,4-dinitrophenylhydrazine and processed for Western blot analysis (50). The degree of protein carbonylation was determined after normalization with the amount of loaded proteins, evaluated by densitometry of the Ponceau red staining. Whenever possible, two different homogenate preparations from each biopsy were assayed for Oxyblot analysis, and mean values of normalized protein carbonylation were used for statistical analysis.

Western blot analysis was performed using chemiluminescence detection, as previously described (9, 46), using the following mouse monoclonal antibodies as primary antibodies: anti-generic MHC, BF-46 (9); anti-α-sarcomeric actin, 5C5 (Sigma, Milano, Italy); anti-tropomyosin, CH1 (Sigma); anti-Grp75 (SPS-825, Stressgen); and anti-HO-1 antibody (OSA-110; Stressgen). After extensive rinses with Tris-buffered saline-Tween, filters were incubated with appropriate dilution of anti-mouse immunoglobulins conjugated with peroxidase (sc-2005; Santa Cruz Biotechnology) 1:4000 in blocking reagent (BR) 0.5% in Tris-buffered saline-Tween. Peroxidase activity was revealed using chemiluminescence (ECL, GE Healthcare, Little Chalfont, UK).

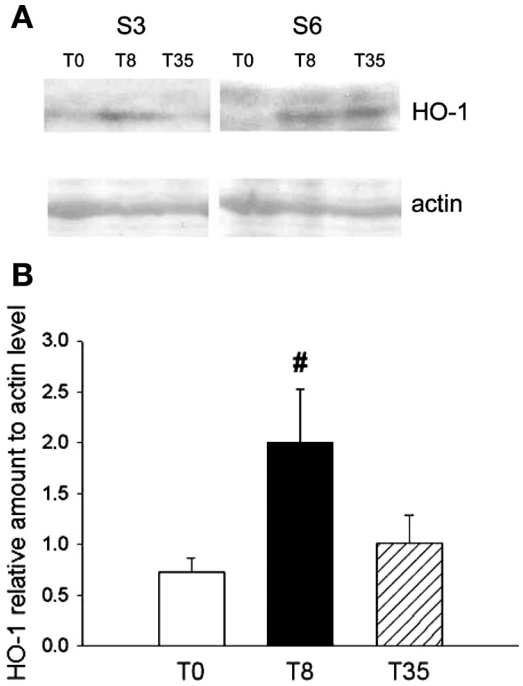

Fig. 3. Bed rest-induced changes in muscle heme oxygenase-1 (HO-1) protein levels. *A*: representative WB from biopsies obtained at T0, T8, or T35 of bed rest from different subjects labeled with antibodies for HO-1. RP staining of actin is shown as a reference for sample loading. *B*: histograms show means and SE of the relative amount of HO-1 levels to actin levels from biopsies obtained at different times ($n = 8$ subjects). #Significant difference vs. T0 sample only ($P < 0.05$, within-subjects ANOVA).

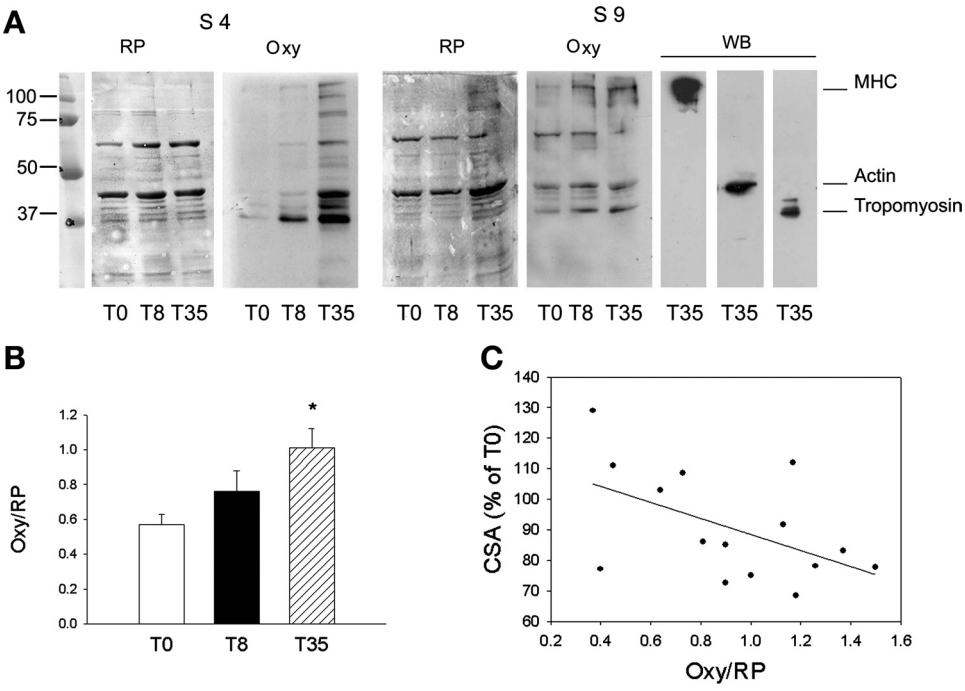

Fig. 2. Bed rest-induced changes in muscle protein carbonylation. *A*: representative red Ponceau (RP) stainings and Oxyblots (Oxy) of biopsies obtained at T0, T8, or T35 of bed rest from two different subjects. WB indicates parallel Western blots of T35 lysate from S9, labeled with antibodies for myosin heavy chains (MHC), actin, and tropomyosin. Protein molecular weight markers are located on the *left*. *B*: histograms show means and SE of the relative amount of Oxy/RP values from biopsies obtained at T0, T8, and T35 from 8 volunteers. Two subjects (S1 and S2) lacked one biopsy for technical reasons, as described in MATERIAL AND METHODS. *Significant difference ($P < 0.02$, within-subjects ANOVA). *C*: regression analysis of normalized levels of muscle protein oxidation (Oxy/RP) vs. percent change of fiber CSA, determined in T8 and T35 biopsies ($r^2 = 0.26$; $P = 0.04$; see RESULTS for equation details).

Protein levels were quantified via measurement of optical density using the National Institutes of Health Image J analysis software and normalized to the densitometric value of the Ponceau red staining of the corresponding actin band (35).

Experimental rat hindlimb suspension. Hindlimb muscles of 6-wk-old Wistar rats were unloaded using the tail-suspension model (19). The protocol was approved by the Animal Care Committees of the University of Padova and the Italian Ministry of Public Health. Each animal was weighed before and after the suspension period. At least four animals for each group were killed after 1, 4, 7, and 15 days of entry in the experimental protocol. A comparable number of ambulatory rats of the same age and weight were used for control. The day of death, rats were anesthetized and euthanized, and soleus muscles were excised, weighted, and frozen in liquid nitrogen.

Statistical analysis. All data were expressed as means ± SE. Statistical analysis was performed utilizing one-way repeated-measures ANOVA (within-subject ANOVA), with time as repeated factor. Post hoc Bonferroni tests were performed to assess specific differences between times (T0, T8, T35). The paired Student's *t*-test was adopted when only T0 and T35 values were compared. Unpaired analysis (one-way ANOVA and post hoc *t*-test) was adopted for data concerning suspended rats. P value = 0.05 was set as the limit for significance. Data were analyzed by simple linear regression, and a Pearson correlation coefficient (r) was calculated. Analyses were performed using statistical package SigmaStat version 2.0 (Jandel Europe).

RESULTS

Muscle atrophy and protein carbonylation. Whenever compatible with the orientation of muscle fibers in the biopsy, fiber CSA was used to evaluate the degree of atrophy (see Supplemental Table 1, available with the online version of this article). No significant variation of the mean fiber CSA was observed in T8 biopsies, whereas mean fiber CSA value was reduced ~18% compared with T0 value after 5 wk of bed rest (Fig. 1*A*, $P < 0.05$, $n = 7$, within-subjects ANOVA). However, when comparison were performed considering mean CSA values for each fiber population of T35 biopsies, only CSA of slow type 1 fibers and fast type 2X fibers showed a significant reduction, compared with T0 values (Fig. 1*B*, $P = 0.02$ for type 1 fibers; $P = 0.08$ for type 2A fibers, and $P = 0.03$ for type 2X fibers, paired Student's *t*-test). No significant variation in the relative percentage of the number of each fiber-type population was detected in T35 biopsies, compared with T0 values (Table 1).

Protein carbonylation analysis showed variable signal intensity of T8 samples (Fig. 2 and Supplemental Table 1). Conversely, the level of protein carbonylation appeared more consistently increased at T35 (Fig. 2 and Supplemental Table 1). Staining of parallel gels with antibodies specific for myo-

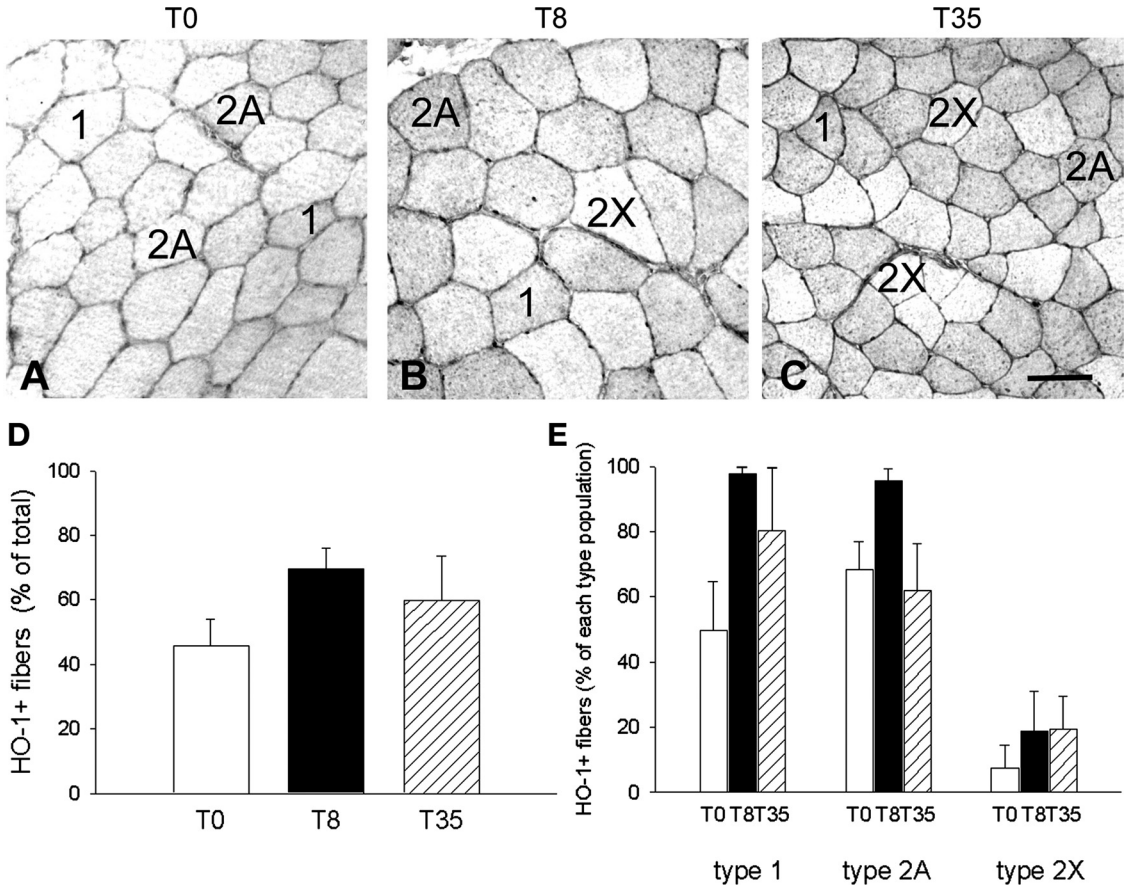

Fig. 4. Bed rest-induced changes in the distribution of HO-1 immunoreactivity among fiber-type populations. *A–C*: representative indirect immunoperoxidase staining of cryosections from biopsies obtained from S10 at T0 (*A*), T8 (*B*), or T35 (*C*) of bed rest with anti-HO-1 antibodies. Labeling with 1, 2A, and 2X indicates the representative HO-1 staining (the presence and/or the absence) within the corresponding fiber type, as determined by comparison of serial sections reacted with isoform-specific anti-MHC antibodies (see MATERIALS AND METHODS). Bar: 50 μm. *D*: the histogram shows means and SE of the absolute percentage of HO-1 positive (+) fibers in T0, T8, and T35 biopsies of S3, S7, and S10 (average no. of muscle fibers evaluated in representative fields for each biopsy = 250). *E*: histogram illustrates the relative percentage of HO-1 + fibers to the fiber number of each type population in T0, T8, and T35 biopsies of the same subjects analyzed in *D*. Values correspond to means and SE (average no. of muscle fibers evaluated in representative fields for each biopsy = 250).

fibrillar proteins showed that MHC, actin, and tropomyosin corresponded in mobility to the most heavily carbonylated species (Fig. 2*A*). Paired statistical analysis indicated that Oxyblot/red Ponceau levels were significantly and about twofold higher at T35, compared with T0 values ($P < 0.02$, $n = 8$; within-subjects ANOVA) (Fig. 2*B*). Figure 2*C* depicts the relation between fiber atrophy and muscle protein oxidation among individual T8 and T35 biopsies. Mean fiber CSA, expressed as the percentage of T0 values, declines in the presence of increased degree of protein carbonylation [regression equation: $y = 114.72–26.26x$, $r^2 = 0.26$; 95% confidence interval (CI): 0.000005 lower limit, 0.63942 upper limit; $P = 0.04$].

Changes in HO-1 protein level and cellular distribution. Western blot analyses performed on whole lysates from biopsies obtained at T0, T8, and T35 showed the presence of significant changes in the total content of HO-1 during bed rest (Fig. 3 and Supplemental Table 1). Increased signals for HO-1 levels were consistently observed in T8 biopsies, compared with T0; conversely, signals displayed variable intensity in T35 biopsies (Fig. 3*A*). Densitometric analysis and subsequent normalization to actin levels showed a significant twofold increase in relative HO-1 protein levels at T8, compared with T0 levels ($P < 0.05$; $n = 8$; within-subjects ANOVA), whereas no significant difference was observed compared with T35 levels (Fig. 3*B* and Supplemental Table 1). We then evaluated the distribution of HO-1 immunoreactivity among muscle fiber populations. As described for the rat (46), HO-1 immunoreactivity appeared weakly detectable in a number of type 1 and type 2A fibers of T0 biopsies (Fig. 4). Labeling increased in intensity in T8 biopsies and involved >80% of muscle fibers of the type 1 population (average number of fibers considered for each biopsy of S3, S7, and S10 = 250, Fig. 4, *B* and *E*). The percentage of HO-1 immunoreactive fibers was still high in T35 biopsies, albeit lacking statistical significance (Fig. 4, *C* and *D*), possibly due to the higher sensitivity of the immunohistochemical approach, compared with Western blot analysis.

Changes in Grp75 protein levels and cellular distribution. Similar to what was described for HO-1, Western blot analyses showed increased signals for Grp75 in T8 biopsies, compared with T0, whereas they displayed signals with variable intensity in T35 ones (Fig. 5*A*). Normalization with actin levels showed a significant threefold increase of Grp75 signals in T8 biopsies, compared with both T0 and T35 values ($P < 0.05$ using within-subjects ANOVA, $n = 8$), whereas T35 values did not differ significantly from T0 ones (Fig. 5*B* and Supplemental Table 1). Figure 5*C* depicts the relation between Grp75 levels and fiber atrophy among individual biopsies. Mean fiber CSA, expressed as the percentage of T0 values, is maintained in the presence of the highest increases in Grp75 protein level, expressed as the percentage of T0 values, whereas it declines as Grp75 protein level returns to T0 value (regression equation: $y = 71.92+0.09x$, $r^2 = 0.40$; 95% CI: 0.02 lower limit, 0.74 upper limit; $P = 0.01$; outlayer value of S8 was excluded from this analysis).

At variance with HO-1, immunohistochemical analysis showed that, in T0 biopsies, Grp75 immunoreactivity was apparently absent from the large majority of muscle fibers (Fig. 6*A*), and, when present (not shown), it was very weak

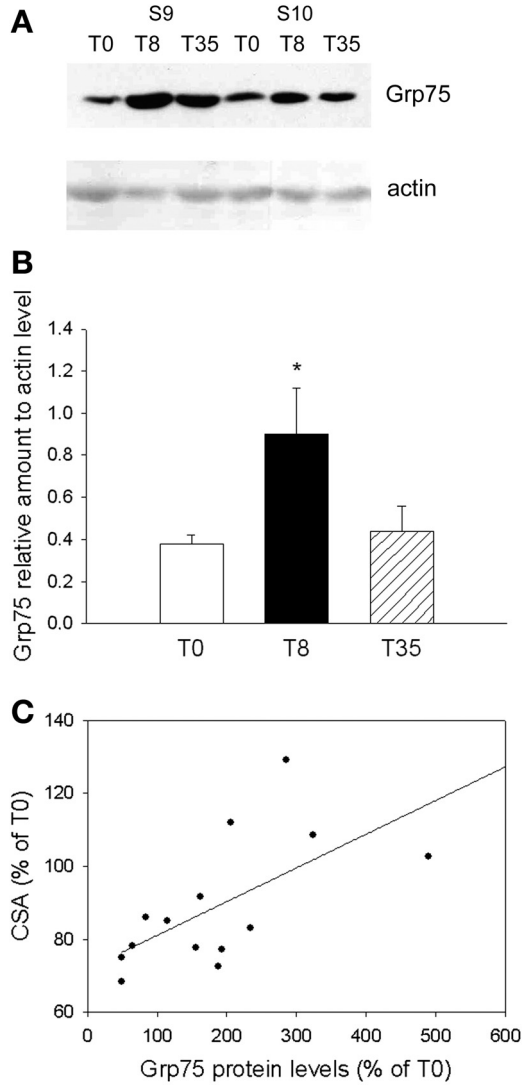

Fig. 5. Bed rest-induced changes in muscle glucose-regulated protein-75 (Grp75) protein levels. *A*: representative WB from biopsies obtained at T0, T8, or T35 of bed rest from different subjects labeled with antibodies for Grp75. Staining of actin is shown as a reference for sample loading. *B*: histograms show means and SE of the relative amount of Grp75 levels to actin levels from biopsies obtained at different times ($n = 8$ subjects). *Significant difference vs. both T0 and T35 samples ($P < 0.05$, within-subjects ANOVA). *C*: regression analysis of the percent change of Grp75 protein level vs. that of fiber CSA, determined in T8 and T35 biopsies ($r^2 = 0.40$; $P = 0.01$; see RESULTS for equation details).

and detected within a small number of type 1 and type 2A fibers (Fig. 6, *D* and *E*). Intensity of Grp75 immunoreactivity increased in T8 biopsies and involved ~50% of muscle fibers (average number of fibers considered for each T8 biopsy of S3, S7, and S10 = 250, $P < 0.025$, within-subjects ANOVA; Fig. 6, *B* and *D*). At T8, reactivity for Grp75 was largely distributed within type 1 fibers ($P < 0.025$, within-subjects ANOVA) and type 2A fiber population ($P < 0.01$, within-subjects ANOVA), whereas type 2X fibers appeared unlabeled (average number of fibers considered for each T8 biopsy of S3, S7, and S10 = 250; Fig. 6, *B* and *E*). The percentage of Grp75 positive fibers significantly declined in T35 biopsies (Fig. 6, *C* and *D*), although staining remained detectable in a number of type 1 fibers

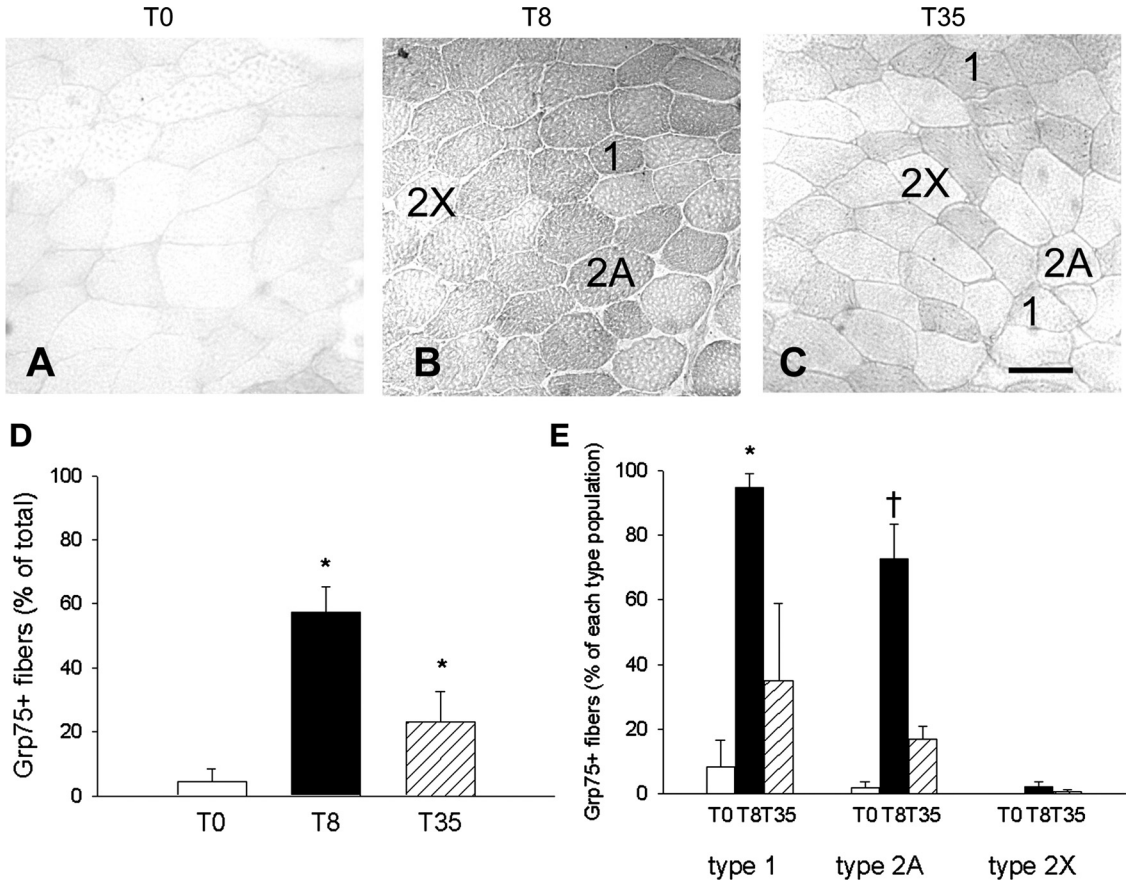

Fig. 6. Bed rest-induced changes in the distribution of Grp75 immunoreactivity among fiber-type populations. *A–C*: representative indirect immunoperoxidase staining of serial adjacent cryostat sections from S7 biopsies obtained at T0 (*A*), T8 (*B*), or T35 (*C*) of bed rest with anti-Grp75 antibody. Labeling with 1, 2A, and 2X indicates the representative Grp75 staining (the presence and/or the absence) within the corresponding fiber type, as determined by comparison of serial sections reacted with isoform-specific anti-MHC antibodies (see MATERIALS AND METHODS). Bar: 50 μm. *D*: histogram shows means and SE of the absolute percentage of Grp75 positive (+) fibers in T0, T8, and T35 biopsies of S3, S7, and S10 (average no. of muscle fibers evaluated in representative fields for each biopsy = 250). *Statistically significant difference ($P \leq 0.05$, within-subjects ANOVA) vs. T0. *E*: histogram illustrates the relative percentage of Grp75 + fibers to the fiber number of each type population in T0, T8, and T35 biopsies of the same subjects analyzed in *D*. Values correspond to means and SE (average no. of muscle fibers evaluated for each biopsy = 250). *Significant difference vs. T0 ($P < 0.025$); †significant difference vs. T0 and T35 ($P < 0.01$, within-subjects ANOVA).

(average number of fibers considered for each T35 biopsy of S3, S7, and S10 = 250; Fig. 6, *C* and *E*).

Changes in Grp75 protein levels in soleus muscle of hindlimb-suspended rats. To confirm that disuse evoked the observed increase of Grp75 expression in human muscle, parallel analyses were performed on soleus muscles of tail-suspended rats, a well-established experimental protocol of severe muscle disuse atrophy (19). Soleus muscle atrophy was evaluated by comparison of the muscle weight-to-body weight ratio (MW/BW) of unloaded and ambulatory rats, and values showed that, after 1 day of unloading, there was a nonsignificant 5% decrease (mean and SE of MW/BW of unloaded and ambulatory soleus, $0.39 \pm 0.011 \times 10^{-3}$ and $0.41 \pm 0.007 \times 10^{-3}$, respectively, $n = 8$, $P = 0.22$, Student's *t*-test). Soleus MW/BW significantly decreased ~14% after 4 days of unloading ($n = 6$; $P = 0.02$), ~28% after 7-day unloading ($n = 12$; $P < 0.0001$), and 40% after 15 days of unloading ($n = 6$; $P < 0.0001$), compared with the respective group of ambulatory soleus muscles (Student's *t*-test). Analysis of fiber CSA was then performed on 1-day unloaded soleus muscles. Only fast fibers showed a significant decrease in CSA, compared with ambulatory muscles (means and SE of fiber CSA of unloaded and ambulatory muscles 1,191 ± 45 and 1,323 ± 36 μm^2, respectively, $P = 0.04$, $n = 6$, n of fast fibers evaluated for each muscle = 100), whereas no significant difference was observed between CSA values of slow ones (mean and SE of fiber CSA of unloaded and ambulatory muscles, 1,623 ± 23 and 1,786 ± 95 μm^2, respectively, $P = 0.18$, $n = 6$, n of slow fibers evaluated for each muscle = 100).

Western blot analysis showed increased Grp75 protein levels in 1-day unloaded soleus muscles, compared with protein levels detected in the soleus muscles of ambulatory rats and of 4- to 15-day suspended ones (Fig. 7, *A* and *B*; $n = 4$, $P = 0.02$, ANOVA). Figure 7*C* depicts the relation between Grp75 protein levels and the degree of muscle atrophy. MW/BW value, expressed as the percentage of the mean value of the corresponding group of ambulatory rats, is maintained in the presence of higher Grp75 protein levels, whereas it declines as Grp75 protein levels decrease (regression equation: $y = 58.04 + 21.63x$, $r^2 = 0.22$; 95% CI: 0.000005 lower limit, 0.5488 upper limit; $P = 0.03$).

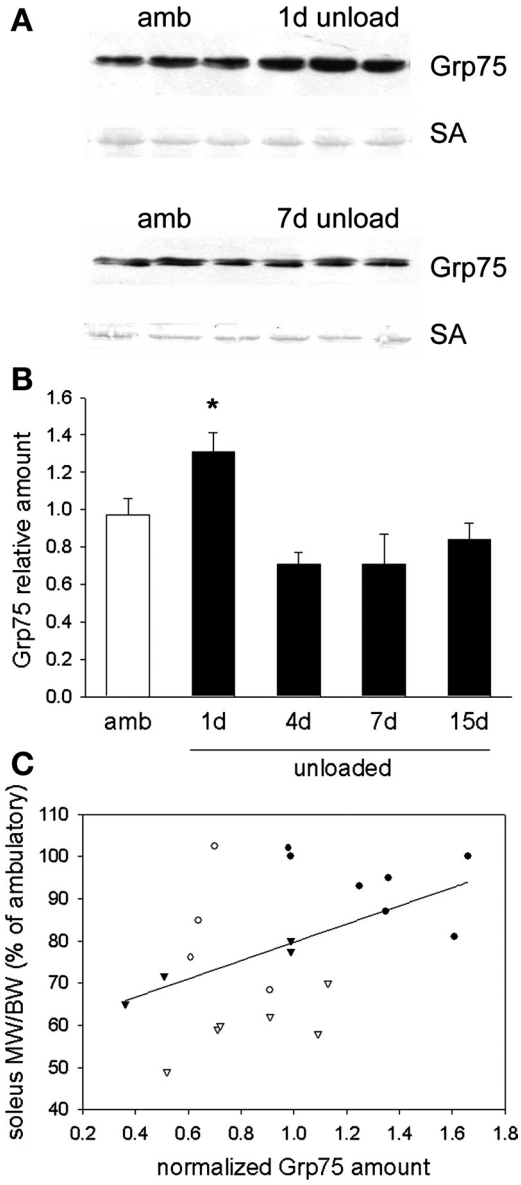

Fig. 7. Hindlimb suspension-induced changes in Grp75 protein levels of rat soleus muscles. *A*: representative WB of soleus muscles obtained from ambulatory rats (amb) and tail-suspended ones (unload) after 1 and 7 days of unloading and labeled with anti-Grp75 antibodies. Staining of serum albumin (SA) is shown as a reference for sample loading, instead of actin, whose amount might be decreased in the presence of severe atrophy. *B*: histograms show means and SE of normalized Grp75 levels to SA obtained from soleus muscles after different unloading times ($n = 4$). *Significant difference vs. ambulatory soleus muscles ($P = 0.02$, ANOVA). *C*: regression analysis of normalized Grp75 protein amount vs. muscle weight-to-body weight ratio (MW/BW) of unloaded soleus muscles, expressed as the percentage of amb values ($r^2 = 0.22$; $P = 0.03$; see RESULTS for equation details). ●, 1-Day unloading; ○, 4-day unloading; ▼, 7-day unloading; ▽, 15-day unloading.

DISCUSSION

This is the first study to show that skeletal muscle atrophy induced in humans by bed rest was accompanied by increased protein carbonylation, a marker of oxidative stress. In addition, muscle disuse during bed rest was characterized by an early, albeit transient, increase in the expression of two stress proteins involved in the antioxidant protection, such as HO-1 and Grp75. A transient increase in Grp75 expression was detected also in the soleus muscle of the tail-suspended rat, before statistically significant evidence of muscle atrophy.

Among the possible different factors that contribute to the development of muscle atrophy (i.e., decreased protein synthesis, increased protein degradation, increased myonuclear apoptosis; Refs. 2, 25, 38, 45), a promoting role has been proposed for oxidative stress (36), based on the increasing body of evidence, collected from animal experimental models and concerning oxidant-induced posttranslational and transcriptional changes on muscle proteins and genes (3, 17, 21–23). Although the source of ROS in inactive muscle fibers remains still undetermined, the reduced activity or the imbalance of the level of antioxidant enzymes, such as catalase vs. superoxide dismutase (23, 44, 45), might determine the increase in oxidative stress observed in the disused muscle. In humans, increased levels of oxidative stress markers, such as total glutathione (8) and protein carbonylation (50), were detected in atrophic muscles of patients affected with different pathological conditions. However, these observations were limited by the chance that disease-specific mechanisms contributed to the generation of oxidative stress (8, 50). Data obtained from this investigation exclude the contribution of disease-related influences and show that oxidative stress, revealed by muscle protein carbonylation, is increased by disuse in humans, similarly to what occurs during muscle inactivity in experimental animal models (3, 21, 36). The degree of muscle protein carbonylation significantly increased with the decrease of fiber CSA, although the low value of the r^2, probably determined by the small number of the subjects studied, would rather indicate a trend toward a negative correlation. Nevertheless, our result is consistent with the finding of a negative correlation between muscle mass and oxidant production reported for murine soleus muscles made atrophic by hindlimb unloading (3).

Oxidative injury might affect both protein conformation, taking to the loss of the biological function (9) and the dismissal to the degradation pathway (36, 38), and protein synthesis, through RNA oxidation, possibly mediated by increased non-heme iron (17). Furthermore, ROS increase the transcription of translational inhibitors (45) and the activity of atrophy gene regulators, such as forkhead box 3a and NF-κB (13, 26). Therefore, oxidative stress appears to act upstream of the major mechanisms contributing to skeletal muscle atrophy, i.e., the increase in protein degradation and the changes in protein synthesis, which would result from the specific transcription of proatrophic genes (38) and the direct injury of ROS on RNAs (17).

In addition, ROS can evoke an antioxidant stress response (18). Although several investigations using experimental animal models of disuse atrophy showed a decrease in the expression of Hsp (32–33, 45), a different behavior was displayed by HO-1, a small Hsp detectable at low levels in skeletal muscle, which increased after muscle disuse due to hindlimb suspension or to mechanical ventilation (12, 18). The present study shows that muscle disuse, induced in vastus lateralis by 1 wk of bed rest, is characterized by the significant and transient increase of both HO-1 and Grp75 protein levels, two stress proteins that are upregulated by and able to counteract oxidative stress (10, 20, 37). Differently from HO-1, the increase of Grp75 protein levels in disused muscle has never been reported

before. Grp75, known either as mitochondrial Hsp70, mortalin, or peptide-binding protein 74, is an Hsp70 analog prevalently localized within mitochondria and endoplasmic reticulum (20). Grp75 protein levels increased in mitochondria after exposure of endothelial cells to hydrogen peroxide (30), and in human muscle after training of both high and low intensity (14, 48), being, at the same time, upregulated by and protective against oxidative stress (20, 27, 48). A positive correlation was reported between Grp75 muscle levels and aerobic exercise capacity in trained subjects with impaired glucose tolerance (48). Here we showed that, during bed rest, the extent of upregulation of this protein depicted a significant linear correlation with the percent change in fiber CSA, in that increased Grp75 expression was observed in the presence of maintenance of the fiber CSA, whereas the lack of increase or the reduction of Grp75 protein amount to prebed rest levels was detected in the presence of muscle atrophy. In fact, muscle Grp75 levels increased significantly at T8, to decrease at T35, when they returned to prebed rest levels. Comparable results on transient Grp75 upregulation were also observed in an experimental animal model of muscle disuse. Hindlimb suspension in the rat induced quickly a severe atrophy of the anti-gravitational muscles, due to the higher protein turnover of this species compared with humans (51). Consistently with the higher metabolic rate, the transient increase in Grp75 expression of the soleus muscle occurred already after 24 h of unloading and in the absence of a statistically significant reduction in MW/BW and in slow fiber CSA. In 1-day unloaded muscles, CSA decrease affected significantly only fast fibers, which represented a minor proportion of soleus muscle fibers (about 13% in 6-wk-old rats).

Also Grp75 levels detected in disused rat soleus muscle significantly correlated with the maintenance of soleus muscle mass, albeit the regression analysis showed a lower r^2 value than that one observed when correlating Grp75 protein levels and fiber CSA of the biopsies of bed-rest volunteers.

The increased expression of HO-1 and Grp75 in muscle appears to be circumscribed to the first week(s) of bed rest. It remains still obscure, the mechanism, through which muscle disuse blunts this stress response. Although there are examples that a stress response may be maintained for a long time (46), it is soon switched off. Possible mechanisms are quenching of the stressing stimulus by the stress protein themselves and/or the upregulation of translational inhibitors, which was detectable already after 1 day of unloading in the soleus muscle of hindlimb-suspended rats (45).

We wonder whether the cytoprotective properties of these two stress proteins contribute to the antioxidant defense of disused muscle fibers. Upregulation of other stress proteins, like Hsp70, induced either by heat stress or by genetic manipulation, was shown to prevent the development of muscle disuse atrophy in experimental animals (32, 41) by inhibiting the activity of forkhead box 3a and NF-κB (41). Immunohistochemistry showed that, in humans, HO-1 expression localized within skeletal muscle fibers, as described for rat hindlimb muscles (46), being detectable in the large majority of type 1 and 2A ones. Because during bed rest the proportion of HO-1 positive fibers did not change significantly, along with the increase in the corresponding protein level, nor the positive staining involved type 2X fibers, we hypothesize that the increase in HO-1 expression occurred within these two fiber populations. Interestingly, also Grp75 immunoreactivity localized within these same fiber populations, albeit transiently, in T8 biopsies. Such a distribution suggests that type 1 and 2A fibers of T8 biopsies experienced oxidative stress, possibly in relation to their high mitochondrial content. It is worth noting that training also induced a higher expression of Grp75 in muscles with slower MHC profile (48).

Other effectors of the antioxidant defense may participate in delaying the progression of muscle atrophy, being recruited at subsequent times. Additional data of ours, obtained from the same volunteers participating in the bed-rest protocol, indicate that glutathione appeared to be enrolled later on, i.e., glutathione synthesis rate increased in T35 biopsies and negatively correlated with muscle atrophy levels (F. Agostini, L. Dalla Libera, J. Rittweger, S. Mazzucco, M. Jurdana, G. Guarnieri, I. B. Mekjavic, R. Pišot, L. Gorza , M. Narici and G. Biolo, unpublished observations). The finding that glutathione levels decreased in the presence of severe muscle fiber atrophy (~55%), induced in the diaphragm by mechanical ventilation (25), supports further the hypothesis that antioxidant defenses (stress proteins and antioxidants) may counteract the onset and the progression of muscle atrophy.

We conclude that, in humans, as shown for rodents, disuse muscle atrophy is characterized by the increase of muscle protein carbonylation and by the blunted expression of stress proteins involved in the antioxidant defense. Future investigations aimed to identify the mechanism(s) responsible for the switching off of this stress response would clarify whether its persistence would rescue disused muscle fibers against the increase in protein oxidation and the decrease in myofiber size.

ACKNOWLEDGMENTS

We thank the volunteers, who gave their time and effort to ensure the success of this project. We acknowledge the excellent assistance of the entire staff of the Valdoltra Orthopaedic Hospital of Ankaran (Koper, Slovenia).

GRANTS

The financial support of the Agenzia Spaziale Italiana is gratefully acknowledged (Grants OSMA-WP1B51-2 to L. Gorza and OSMA-WP1B52-1 to G. Biolo).

REFERENCES

1. **Adams GR, Caiozzo VJ, Baldwin KM.** Skeletal muscle unweighting: spaceflight and ground-based models. *J Appl Physiol* 95: 2185–2201, 2003.
2. **Allen DL, Linderman JK, Roy RR, Bigbeee AJ, Grindeland RE, Mukku V, Egerton VR.** Apoptosis: a mechanism contributing to remodeling of skeletal muscle in response to hindlimb unweighting. *Am J Physiol Cell Physiol* 273: C579–C587, 1997.
3. **Arbogast S, Smith J, Matuszczak Y, Hardin BJ, Moylan JS, Smith JD, Ware J, Kennedy AR, Reid MB.** Bowman-Birk inhibitor concentrate prevents atrophy, weakness, and oxidative stress in soleus muscle of hindlimb-unloaded mice. *J Appl Physiol* 102: 956–964, 2007.
4. **Barker T, Traber MG.** From animals to humans: evidence linking oxidative stress as a causative factor in muscle atrophy. *J Physiol* 583: 221–222, 2007.
5. **Berg HE, Larsson L, Tesch PA.** Lower limb skeletal muscle function after 6 wk of bed rest. *J Appl Physiol* 82: 182–188, 1997.
6. **Biolo G, Agostini F, Simunic B, Sturma M, Torelli L, Preiser JC, Deby-Dupont G, Magni P, Strollo F, di Prampero P, Guarnieri G, Mekjavic IB, Pišot R, Narici M.** Positive energy balance is associated to accelerated muscle atrophy and increased erythrocyte glutathione turnover during 5 wk of bed rest. *Am J Clin Nutr* 88: 950–958, 2008.
7. **Blottner D, Salanova M, Püttmann B, Schiffl G, Felsenberg D, Buehring B, Rittweger J.** Human skeletal muscle structure and function

preserved by vibration muscle exercise following 55 days of bed rest. *Eur J Appl Physiol* 97: 261–271, 2006.
8. **Crowe AV, McArdle A, McArdle F, Patweel DM, Bell GM, Kemp GJ, Bone JM, Griffiths RD, Jackson MJ.** Markers of oxidative stress in the skeletal muscle of patients on haemodialysis. *Nephrol Dial Transplant* 22: 1177–1183, 2007.
9. **Dalla Libera L, Ravara B, Gobbo V, Danieli Betto D, Germinario E, Angelini A, Vescovo G.** Skeletal muscle myofibrillar protein oxidation in heart failure and the protective effect of Carvedilol. *J Mol Cell Cardiol* 38: 803–807, 2005.
10. **Datla SR, Dusting GJ, Mori TA, Taylor CJ, Croft KD, Jiang F.** Induction of heme oxygenase-1 in vivo suppresses NADPH oxidase-derived oxidative stress. *Hypertension* 50: 636–642, 2007.
11. **de Boer MD, Seynnes OR, di Prampero PE, Pišot R, Mekjavic IB, Biolo G, Narici MV.** Effect of 5 weeks horizontal bed rest on human muscle thickness and architecture of weight bearing and non-weight bearing muscles. *Eur J Appl Physiol* 104: 401–407, 2008.
12. **DeRuisseau KC, Shanely RA, Akunuri N, Hamilton MT, Van Gammeren D, Zergeroglu AM, McKenzie M, Powers SK.** Diaphragm unloading via controlled mechanical ventilation alters the gene expression profile. *Am J Respir Crit Care Med* 172: 1267–1275, 2005.
13. **Furukawa-Hibi Y, Yoshida-Araki K, Ohta T, Ikeda K, Motoyama N.** FOXO forkhead transcription factors induce G(2)-M checkpoint in response to oxidative stress. *J Biol Chem* 277: 26729–26732, 2002.
14. **Gjøvaag TF, Dahl HA.** Effect of training and detraining on the expression of heat shock proteins in m. triceps brachii of untrained males and females. *Eur J Appl Physiol* 98: 310–322, 2006.
15. **Gorza L.** Identification of a novel type 2 fiber population in mammalian skeletal muscle by combined use of histochemical myosin ATPase and anti-myosin monoclonal antibodies. *J Histochem Cytochem* 38: 257–265, 1990.
16. **Gorza L, Menabò R, Di Lisa F, Vitadello M.** Troponin T cross-linking in human apoptotic cardiomyocytes. *Am J Pathol* 150: 2087–2098, 1997.
17. **Hofer T, Marzetti E, Xu J, Seo AY, Gulec S, Knutson MD, Leeuwenburgh C, Dupont-Versteegden EE.** Increased iron content and RNA oxidative damage in skeletal muscle with aging and disuse atrophy. *Exp Gerontol* 43: 563–570, 2008.
18. **Hunter RB, Mitchell-Felton H, Essig DA, Kandarian SC.** Expression of endoplasmic reticulum stress proteins during skeletal muscle disuse atrophy. *Am J Physiol Cell Physiol* 281: C1285–C1290, 2001.
19. **Jaspers SR, Tischler ME.** Atrophy and growth failure of rat hindlimb muscles in tail-cast suspension. *J Appl Physiol* 57: 1472–1479, 1984.
20. **Kaul SC, Deocaris CC, Wadhwa R.** Three faces of mortalin: a housekeeper, guardian and killer. *Exp Gerontol* 42: 263–274, 2007.
21. **Koesterer TJ, Dodd SL, Powers S.** Increased antioxidant capacity does not attenuate muscle atrophy caused by unweighting. *J Appl Physiol* 93: 1959–1965, 2002.
22. **Kondo H, Miura M, Itokawa Y.** Oxidative stress in skeletal muscle atrophied by immobilization. *Acta Physiol Scand* 142: 527–528, 1991.
23. **Kondo H, Miura M, Itokawa Y.** Antioxidant enzyme systems in skeletal muscle atrophied by immobilization. *Pflügers Arch* 422: 404–406, 1993.
24. **Larsson L, Li X, Berg HE, Frontera WR.** Effects of removal of weight-bearing function on contractility and myosin isoform composition in single human skeletal muscle cells. *Pflügers Arch* 432: 320–328, 1996.
25. **Levine S, Nguyen T, Taylor N, Friscia ME, Budak MT, Rothenberg P, Zhu J, Sachdeva R, Sonnad S, Kaiser LR, Rubinstein NA, Powers SK, Shrager JB.** Rapid disuse atrophy of diaphragm fibers in mechanically ventilated humans. *N Engl J Med* 358: 1327–1335, 2008.
26. **Li H, Malhotra S, Kumar A.** Nuclear factor-kappa B signaling in skeletal muscle atrophy. *J Mol Med* 86: 1113–1126, 2008.
27. **Liu Y, Liu W, Song XD, Zuo J.** Effect of GRP75/mthsp70/PBP74/mortalin overexpression on intracellular ATP level, mitochondrial membrane potential and ROS accumulation following glucose deprivation in PC12 cells. *Mol Cell Biochem* 268: 45–51, 2005.
28. **Margaritis I, Rousseau AS, Marini JF, Chopard A.** Does antioxidant system adaptive response alleviate related oxidative damage with long term bed rest? *Clin Biochem* 42: 371–379, 2009.
29. **Marin-Corral J, Minguella J, Ramírez-Sarmiento AL, Hussain SNA, Gea J, Barreiro E.** Oxidized proteins and superoxide anion production in the diaphragm of severe COPD patients. *Eur Respir J* 33: 1309–1319, 2009.
30. **Mitsumoto A, Takeuchi A, Okawa K, Nakagawa Y.** A subset of newly synthesized polypeptides in mitochondria from human endothelial cells exposed to hydroperoxide stress. *Free Radic Biol Med* 32: 22–37, 2002.
31. **Motterlini R.** Heme oxygenase-1: a key step in counteracting cellular dysfunction. *Cell Mol Biol* 51: 343–346, 2005.
32. **Naito H, Powers SK, Demirel HA, Sugiura T, Dodd SL, Aoki J.** Heat stress attenuates skeletal muscle atrophy in hindlimb-unweighed rats. *J Appl Physiol* 88: 359–363, 2000.
33. **Oishi Y, Ogata T, Yamamoto KI, Terada M, Ohira T, Ohira Y, Taniguchi K, Roy RR.** Cellular adaptations in soleus muscle during recovery after hindlimb unloading. *Acta Physiol (Oxf)* 192: 381–395, 2008.
34. **Pavy-Le Traon A, Heer M, Narici MV, Rittweger J, Vernikos J.** From space to Earth: advances in human physiology from 20 years of bed rest studies (1986–2006). *Eur J Appl Physiol* 101: 143–194, 2007.
35. **Pizzo P, Scapin S, Vitadello M, Florean C, Gorza L.** Grp94 acts as a mediator of curcumin-induced anti-oxidant defence in myogenic cells. *J Cell Mol Med.* In press.
36. **Powers SK, Kavazis AN, McClung JM.** Oxidative stress and disuse muscle atrophy. *J Appl Physiol* 102: 2389–2397, 2007.
37. **Ryter SW, Alam J, Choi AMK.** Heme oxygenase-1/carbon monoxide: from basic science to therapeutic applications. *Physiol Rev* 86: 583–650, 2006.
38. **Sacheck JM, Hyatt JPK, Raffaello A, Jagoe RT, Roy RR, Edgerton VR, Lecker SH, Goldberg AL.** Rapid disuse and denervation atrophy involve transcriptional changes similar to those of muscle wasting during systemic diseases. *FASEB J* 21: 140–155, 2007.
39. **Salanova M, Schiffl G, Rittweger J, Felsenberg D, Blottner D.** Ryanodine receptor type-1 (RyR1) expression and protein *S*-nitrosylation pattern in human soleus myofibres following bed rest and exercise countermeasure. *Histochem Cell Biol* 130: 105–118, 2008.
40. **Schiaffino S, Gorza L, Sartore S, Saggin L, Ausoni S, Vianello M, Gundersen K, Lomo T.** Three myosin heavy chain isoforms in type 2 skeletal muscle fibers. *J Muscle Res Cell Motil* 10: 197–205, 1989.
41. **Senf SH, Dodd SL, McClung JM, Judge AR.** Hsp70 overexpression inhibits NF-κB and Foxo3a transcriptional activities and prevents skeletal muscle atrophy. *FASEB J* 22: 3836–3845, 2008.
42. **Serrano L, Perez M, Lucia A, Chicharro JL, Quiroz-Rothe E, Rivero JLL.** Immunolabelling, histochemistry and in situ hybridisation in human skeletal muscle fibres to detect myosin heavy chain expression at the protein and mRNA level. *J Anat* 199: 329–337, 2001.
43. **Smerdu V, Karsch-Mizrachi I, Campione M, Leinwand L, Schiaffino S.** Type IIx myosin heavy chain transcripts are expressed in type IIb fibers of human skeletal muscle. *Am J Physiol Cell Physiol* 267: C1723–C1728, 1994.
44. **Stein TP.** Space flight and oxidative stress. *Nutrition* 18: 867–871, 2002.
45. **Stevenson EJ, Giresi PG, Koncarevic A, Kandarian SC.** Global analysis of gene expression patterns during disuse atrophy in rat skeletal muscle. *J Physiol* 551: 33–48, 2003.
46. **Tarricone E, Scapin C, Vitadello M, Esposito F, MargonatoV, Milano G, Samaja M, Gorza L.** Cellular distribution of Hsp70 expression in rat skeletal muscles. Effects of moderate exercise training and chronic hypoxia. *Cell Stress Chaperones* 13: 483–495, 2008.
47. **van der Velden J.** Functional significance of myofilament protein oxidation. *Eur Heart J* 27: 764–765, 2006.
48. **Venojärvi M, Aunola S, Puhke R, Marniemi J, Hämäläinen H, Halonen JP, Lindström J, Rastas M, Hällsten K, Nuutila P, Hänninen O, Atalay M.** Exercise training with dietary counselling increases mitochondrial chaperone expression in middle-aged subjects with impaired glucose tolerance. *BMC Endocr Disord* 8: 3, 2009.
49. **Vescovo G, Dalla Libera L, Serafini F, Leprotti C, Facchin M, Volterrani M, Ceconi C, Ambrosio GB.** Improved exercise tolerance after losartan and enalapril in heart failure: correlation with changes in skeletal muscle myosin heavy chain composition. *Circulation* 98: 1742–1749, 1998.
50. **Vescovo G, Ravara B, Dalla Libera L.** Skeletal muscle myofibrillar protein oxidation and exercise capacity in heart failure. *Basic Res Cardiol* 103: 285–290, 2008.
51. **Waterlow JC.** Protein turnover in the whole animal. *Invest Cell Pathol* 3: 107–119, 1980.